

Effect of precursor ratios on the synthesis of MgAl_2O_4 nanoparticles by a reverse microemulsion method

J. Chandradass* and Ki Hyeon Kim*

Department of Physics Yeungnam University Gyeongsan, Gyeongsangbuk-do-712-749 South Korea

The effect of the Mg/Al ratio on the synthesis of MgAl_2O_4 nanoparticles by a reverse micelle process has been investigated in order to identify the phase composition in this system. Our study shows that the precursor ratio has significant effects on the structure and composition of the resulting nanoparticles. From the XRD analysis, a well-crystallized MgAl_2O_4 phase was formed at Mg/Al = 0.5 whereas at Mg/Al = 1, the crystallization of the nanoparticles was sluggish with MgAl_2O_4 and $\theta\text{-Al}_2\text{O}_3$ phases co-existing. By optimizing the Mg/Al ratio in the micelle solution, the average particle size of MgAl_2O_4 nanoparticles as determined from SEM and TEM were found to be 18 and 14 nm, respectively. The FTIR spectra show the lower frequency bands are assigned to metal-oxygen bonds (M-O-M). The thermal behavior of the precursor powders was characterized by DTA-TGA analysis.

Key words: Chemical synthesis, Ceramics: X-ray diffraction, Differential thermal analysis, Thermo gravimetric analysis, Transmission electron microscopy, Fourier transform infrared spectroscopy.

Introduction

Magnesium aluminate spinel (MgAl_2O_4) is one of the best known and widely used polycrystalline materials. It possesses a good combination of features such as high melting point, good mechanical strength, low dielectric constant and high resistance against both alkalis as well as acids [1]. This makes it popular in many industrial applications, e.g., in chemistry, metallurgy and electronics. Chemical inertness makes it an ideal candidate for ultra filtration membranes [2]. Polycrystalline MgAl_2O_4 also finds application as a humidity sensor [3] and an insulating material for fusion reaction cores [4]. Another field of possible uses opens with the fabrication of transparent MgAl_2O_4 ceramics. In this form it is attractive alternative to relatively expensive and difficult to produce MgAl_2O_4 monocrystals. Optical applications of transparent spinels include infra-red windows and a passive Q-switch for lasers [5]. The solid-state synthesis of MgAl_2O_4 spinel requires a higher temperature and longer reaction time so that the synthesized powder suffers from agglomeration and low sintering activity. To tackle these problems, various non-conventional techniques such as; sol-gel, co-precipitation, spray drying, a carbonate precursor method, a citrate-nitrate combustion route, a sucrose method, hydrothermal assisted sol-gel processing, a molten salt method and a microwave assisted combustion synthesis method have been developed for spinel synthesis [6-14].

Although these synthesis routes have been used to synthesize nanoparticles with controlled morphology and structures, and the use of reverse microemulsions seems especially suited for tailoring particle size at the nanolevel [15] Reverse microemulsion system consists of an oil phase, a surfactant, and an aqueous phase. It is a thermodynamically stable isotropic dispersion of the aqueous phase in the continuous oil phase [16]. The advantage of the microemulsion-based route is that it is a soft technique, i.e., it does not require extreme conditions of pressure and temperature. But it is the dynamics of micellar dispersions that makes them so relevant for this kind of purpose: the droplets are indeed subject to Brownian motion and collide continuously, leading to the formation of short-lived dimers and to the exchange of the aqueous contents of the micelles. This dynamic process ensures a homogeneous repartition of the reactants among the aqueous droplets or 'water pools', and thus the formation of very monodisperse particles [17]. In this paper, we report the influence of precursor ratios on the synthesis of MgAl_2O_4 nanoparticles by reverse micelle processing.

Experimental Procedure

In the present study, the following reagents were used for sample preparation. Magnesium (III) nitrate hexahydrate (Sigma Aldrich, USA), Aluminium nitrate nonhydrate (Sigma Aldrich, USA), Cyclohexane (Sigma Aldrich, USA), Poly (oxyethylene) nonylphenyl ether (Igepal CO-520, Aldrich Chemical Co., USA), and NH_4OH (28%) (Dae Jung chemicals, Korea). All reagents were used without further purification. Reverse microemulsion solution was prepared by mixing 40 ml of nonionic surfactant poly (oxyethylene)

*Corresponding author:
Tel : +82-53-810-2334
Fax: +82-53-810-4616
E-mail: anthony_iitm@yahoo.com; keel1@ynu.ac.kr

nonylphenyl ether, 100 ml of cyclohexane and mixed aqueous solution ($Mg/Al = 0.5$ and 1). The microemulsion was mixed rapidly, and after 5 minutes of equilibration, 3-6 ml of NH_4OH was injected into the microemulsion. The microemulsion was then centrifuged to extract the particles, which were subsequently washed by ethanol to remove any residual surfactant. The phase identification of calcined powders was recorded by an X-ray diffractometer (Philips X'pert MPD 3040). Transmission electron microscopy (TEM) was performed at an accelerating voltage of 200 kV, by placing the powder on a copper grid to observe the morphology and size of the powders. The particle size of the calcined powder particles was also observed using a scanning electron microscope (Mira II LMH) at an accelerating voltage of 20 kV. The Fourier transform infrared spectra (FTIR) were measured on a Nicolet Impact 410 DSP spectro-photometer using the KBr pellet method. The thermal characteristics of the precursors were determined by thermogravimetry and differential thermal analysis (STA 1500) in an oxygen atmosphere up to 1400 °C at a heating rate of 10°K minute⁻¹.

Results and Discussion

Many studies of the nanoparticle formation process in reverse micelles have been based on a two-step model [18-20]. The first step is nucleation. The second step is growth via reagent exchanges between micelles. The nucleation and growth are controlled by interaction between micelles, and they can also be affected by the phase behavior and solubility, average occupancy of reacting species in the aqueous medium, dynamic behavior of the reverse micelle solution etc [21].

Fig. 1 shows the X-ray diffraction patterns of precursor powders calcined at 1000 °C with different precursor ratio. The powders obtained from the precursor ratio of $Mg/Al = 0.5$ developed a well-crystallized $MgAl_2O_4$ spinel

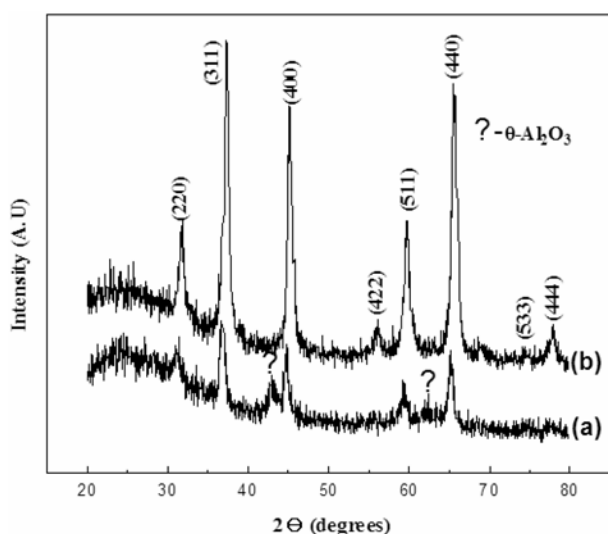


Fig. 1. X-ray diffraction patterns of powders calcined at (a) 1000 °C ($Mg : Al = 1 : 1$); (b) $Mg : Al = 1 : 2$.

phase whereas with a precursor ratio of $Mg/Al = 1$, the crystallization of the nanoparticles was sluggish with $MgAl_2O_4$ and $\theta-Al_2O_3$ phases co-existing.

Fig. 2 show SEM micrographs of the nanopowders obtained at 1000 °C for 2 h with different precursor ratios. It can be seen that nanoparticles are nearly spherical in shape. The narrow size distribution of these nanoparticles is uniform with a regular shape. It follows that the average size of the nanoparticles at $Mg/Al = 0.5$ and 1 are 18 nm and 13 nm respectively. TEM micrographs of the nanopowders obtained at 1000 °C for 2 h with different precursor ratios are shown in Fig. 3. The average particle size at $Mg/Al = 0.5$ is 14 nm whereas at $Mg/Al = 1$, highly agglomerated particles are obtained. It should be mentioned that the size of the particles formed in the reverse micelles is larger than the hydrodynamic size of the reverse micellar droplets in which the particles are formed [22]. The particle size of $MgAl_2O_4$ nanoparticles is lower than the results reported in the literature [10, 14, 23-25].

The IR spectra of the calcined nanocrystalline powders in the wave number region from 4000 to 400 cm^{-1} are shown

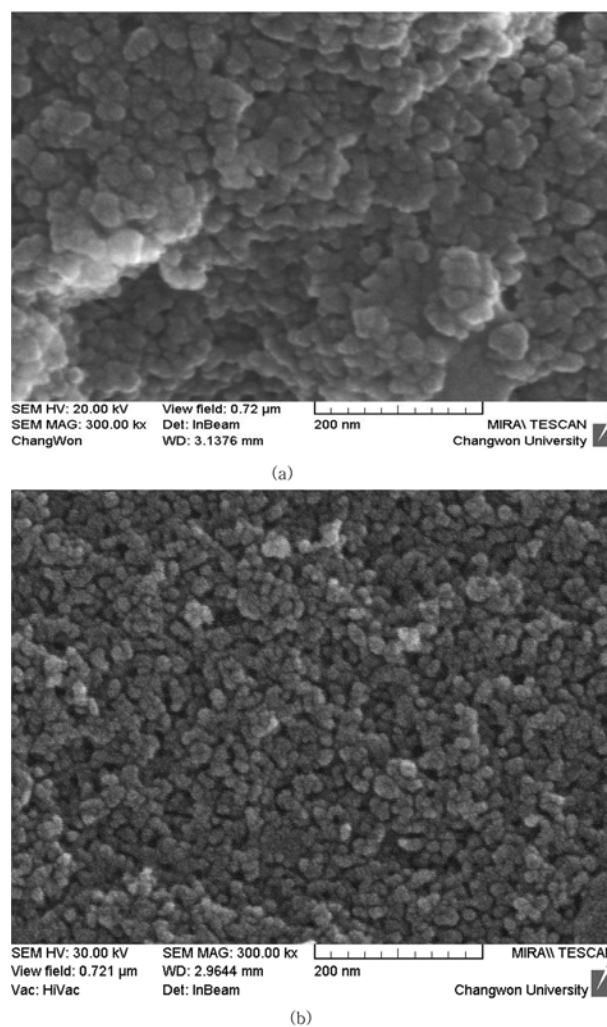


Fig. 2. SEM micrographs of as-synthesized powders calcined at 1000 °C (a) $Mg/Al = 0.5$; $Mg/Al = 1$.

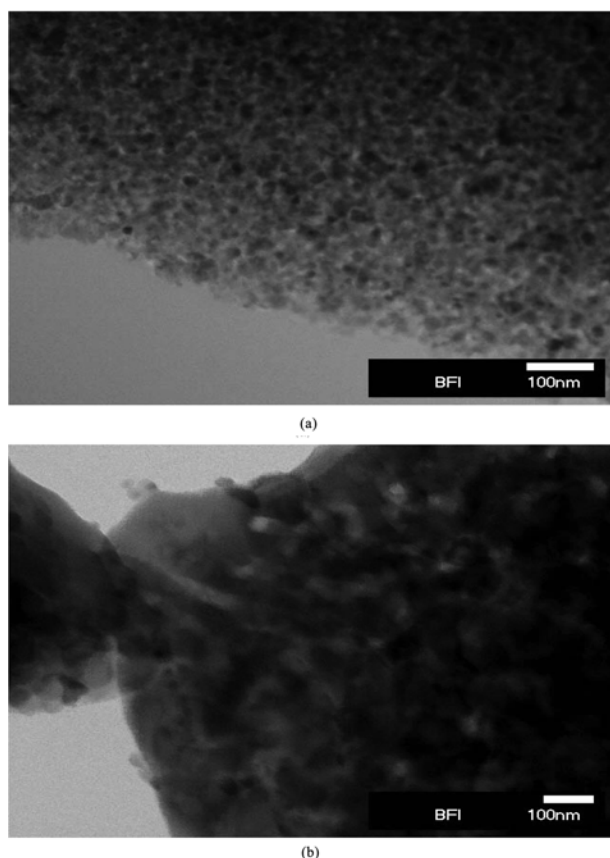


Fig. 3. TEM micrographs of as-synthesized powders calcined at 1000 °C (a) Mg/Al = 0.5; (b) Mg/Al = 1.

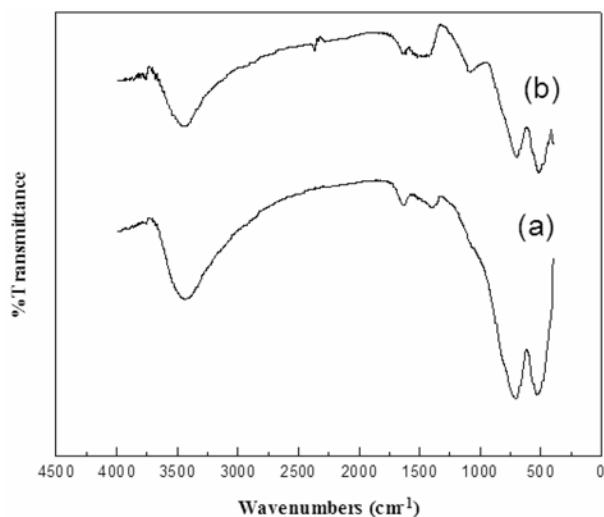


Fig. 4. FTIR analysis of as-synthesized powders calcined at 1000 °C.

in Fig. 4. Absorbance in the range 3200-3700 cm^{-1} is consistent with the O-H stretching of H_2O . The peak around $\sim 2370 \text{ cm}^{-1}$ is typical of CO_2 absorption. The band intensities related to the hydroxyl group and CO_2 band is still visible in the calcined sample. This may be due to moisture absorption during testing. The IR band provides evidence for the presence of organic residuals in the calcined powder in the wave number range of 1300-1400 and 1600-

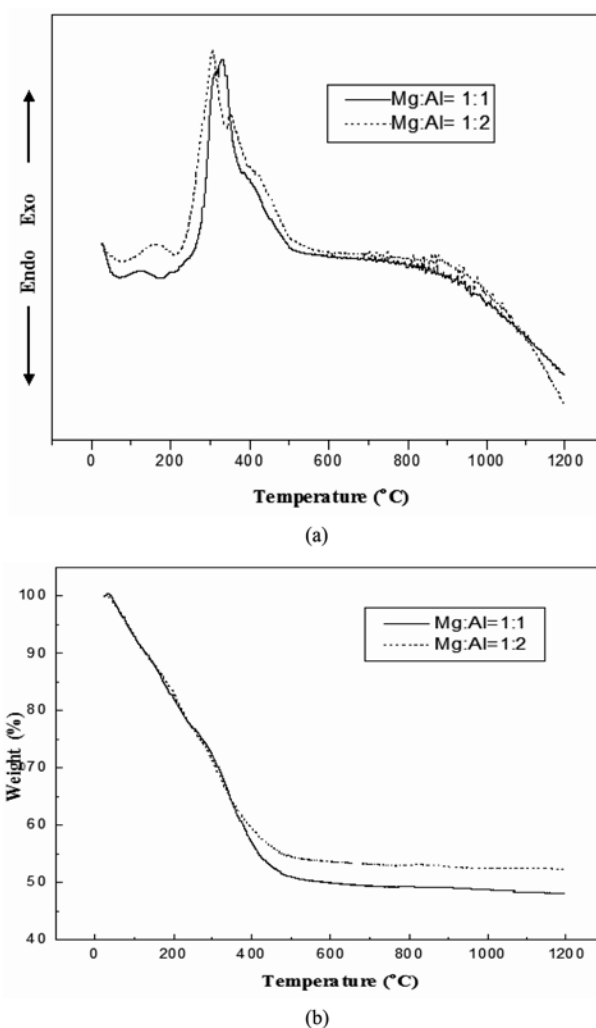


Fig. 5. Thermal analyses of as-prepared powders (a) DTA curves; (b) TGA curves.

1700 cm^{-1} , which corresponds to C-O and C = C stretching vibrations, respectively. The presence of organics in the calcined sample may inhibit the growth of the particle size. The visible band over the range of 1000-400 cm^{-1} corresponds to metal-oxygen bonds (M-O-M) [26, 27].

Thermal behavior of the precursor determined by TG-DTA in oxygen up to 1400 °C at a heating rate of 10 Kminute^{-1} is shown in Fig. 5. Below 150 °C, the weight loss of the sample is about 12% which is caused by the dehydration of the sample; and an endothermic peak in the range 50-60 °C appears in the DTA curve. Between 150-500 °C, the weight loss of the sample is about 37%. This is mainly caused by the combustion of the residual surfactant. Ultimately, an exothermic peak could be observed between 150-500 °C in the DTA curves. The final weight loss ($\sim 2\%$) on the TG curve was observed in the temperature range 500-1400 °C which is due to the removal of residual hydroxyl (OH) group. No clear exothermic peak indicating the transformation temperature to MgAl_2O_4 was observed.

Conclusion

The effect of the Mg/Al ratio on the synthesis of MgAl₂O₄ nanoparticles by a reverse micelle process has been successfully investigated. From the XRD analysis, a well-crystallized MgAl₂O₄ phase was formed at Mg/Al = 0.5. By optimizing the Mg/Al ratio in the micelle solution, the average particle size of MgAl₂O₄ nanoparticles as determined from SEM and TEM were found to be 18 and 14 nm respectively. The FTIR spectra show the lower frequency bands are assigned to metal-oxygen bonds (M-O-M).

References

- M.F.M. Zawrat and A.A. Kheshen, A. A., Br.Ceram. Trans. 101 (2002) 71-74.
- X.L. Pan, S.S. Sheng, G.X. Xiong, K.M. Fang, S. Tudyka and N. Stroh, N, Colloid Surf. A. 179 (2001) 163-169.
- A. Laobuthee, S. Wongkasemjit, E. Traversa and R.M. Laine, J. Eur. Ceram. Soc. 20 (2000) 91-97.
- T. Yano, J. Am.Ceram.Soc. 12 (1999) 3355-3364.
- M.C.L. Patterson, A. DiGiovanni, L. Fehrenbacher and D.W. Roy, Proc. SPIE. 5078 (2003) 71-79.
- G. Ye, G. Oprea and T. Troczynski, J. Am. Ceram. Soc. 88 (2005) 3241-3244.
- N. Thanabodeekij, M. Sathupuya, A.M. Tamieson and S. Wongkasemjit, Mater. Charact. 50 (2003) 325-337.
- E.H. Walker Jr., J.W. Owens, M. Etienne and D. Walker, Mater. Res. Bull. 37(2002) 1041-1050.
- A. Wajler, H. Tomaszewski, E. Drozd-Ciesla and He. Weglarz, J. Eur. Ceram.Soc. 28 (2008) 2495-2500.
- A. Saberi, F. Golestani-Fard, H. Sarpoolaky, M. Willert-Porada, T. Gerdes and R. Reinhard Simon, J Alloy Compd. 462 (2008) 142-146.
- B. Alinejad, H. Sarpoolaky, A. Beitollahi, A. Saberi and S. Afshar, Mater. Res. Bull. 43 (2008) 1188-1194.
- M.M. Amini, M. Mirzaee and N. Sepanj, Mater. Res. Bull. 42 (2007) 563-570.
- D.D. Jayaseelan, S. Zhang, S. Hashimoto and W. Edward Lee, J. Eur. Ceram. Soc. (2007) 4745-4749.
- I. Ganesh, R. Johnson, G.V.N. Rao, Y.R. Mahajan, S.S. Madavendra and B.M. Reddy, Ceram.Int. 31 (2005) 67-74.
- M.P. Pileni (Ed.), Reactivity in Reverse Micelles (Chapters 2, 11, 12), Elsevier, Amsterdam, New York, Oxford, Shannon, Tokyo, 1989, p. 12. T. Sugimoto and K. Kimijima, J. Phys. Chem. B, 107 (2003) 10753-10759.
- T.H. Chieng, L.M. Gan, C.H. Chew and S.C. Ng, Polymer 36 (1995) 1941-1946.
- T.F. Towey, A. Khan-Lidhi and B.H. Robinson, J. Chem. Soc. Faraday Trans. 86 (1990) 3757-3762.
- W. Jahn and R. Strey, J. Phys. Chem. 92 (1988) 2294-2301.
- R. Bandyopadhyaya, R. Kumar, K.S. Gandhi and D. Ramkrishna, Langmuir 13 (1997) 3610-3620.
- M.A. Lopez-Quintela and J. Rivas, J. Colloid Interf. Sci. 158 (1993) 446-451.
- K. Osseo-Asare and F.J. Arriagada, Ceram. Trans. 12 (1990) 3-16.
- N. Munshi, T.K. De and A.N. Maitra, J.Colloid.interf.Sci. 190 (1997) 387-391.
- M.F. Zawrah, H. Hamaad and S. Meky, Ceram. Int. 33 (2007) 969-978.
- G.J. Li, Z.R. Sun, C.H. Chen, X.J. Cui and R.M. Ren, Mater. Lett. 65 (2007) 3585-3588.
- J. Parmentier, M. Richard-Plouet and S. Vilminot, Mater. Res. Bull. 33 (1998) 1717-1724.
- E.G. Brame and J. Grasselli, Infrared and Raman Spectroscopy, Part A, Marcel Dekker, New York, 1976.
- K. Vivekanandan, S. Selvasekarapandian and P. Kollandavel, Mater. Chem. Phys. 39 (1995) 284-289.